Solid-State Amorphization Observed in the Equilibrium-Immiscible Cu−Re System by Molecular Dynamics Simulations

J. H. Li, S. H. Liang, and B. X. Liu*

Advanced Materials Laboratory, Department of Materials Science and Engineering, Tsinghua University, Beijing 100084, China

Received: May 13, 2005; In Final Form: July 8, 2005

Assisted by ab initio calculations, an *n*-body Cu−Re potential is first constructed for the equilibrium-immiscible Cu−Re system under the second moment approximation of a tight-binding scheme. The proven realistic Cu−Re potential is then applied to perform the molecular dynamics simulations using the Cu−Re sandwich model. The simulations reveal that the interfacial free energy stored in the Cu/Re interfaces plays an important role in facilitating the spontaneous solid-state amorphization and that the amorphous interlayer grows in a layer-by-layer mode featuring an asymmetric behavior, i.e., the growth of the amorphous interlayer advances faster toward the Cu lattice than toward the Re direction. It is also found that with increasing the simulation time, the growth speed of the amorphous interlayer gradually slows down and eventually becomes zero when the interlayer reaches a thickness of about 1.47 nm. Interestingly, according to a recently proposed thermodynamic and kinetic model, the maximum thickness of the growing amorphous layer is limited by the available interfacial free energy and in the Cu−Re system, it is estimated to be around 1.35 nm, which is comparable with that observed from the simulations.

I. Introduction

In 1983, Schwarz and Johnson observed, for the first time, a phenomenon called solid-state amorphization (SSA) in the Au−La multilayered films upon thermal annealing at medium temperature, and they claimed that a large negative heat of formation (ΔH_f) and a large atomic size difference between the constituent metals of a binary metal system were necessary for SSA to take place.[1] According to their view, the large negative ΔH_f makes an amorphous phase have a lower free energy than a mechanical mixture of the two polycrystalline metals, thus serving as a major thermodynamic driving force, while the large atomic size difference is responsible for an asymmetric diffusion, i.e., atoms of one metal diffuse abnormally faster into its partner than vice versa, thus suppressing either nucleation or growth of a possible intermetallic compound, frequently of complicated structure. In 1986, Clemens suggested two similar parameters to predict the possibility of SSA, i.e., a large negative ΔH_f and a small atomic volume ratio,[2] resulting in not only an asymmetric diffusion but also a disordered interfacial layer, which could, in turn, provide some nucleation sites for growing an amorphous phase. Since the mid-1990s, however, SSA has been observed experimentally in some binary metal systems with neither a large negative ΔH_f (e.g., the Ni−Mo system) nor a large size difference (e.g., the Au−Ta system).[3,4] Moreover, SSA has even been achieved in several systems with a positive ΔH_f (e.g., the Cu−W system).[5] In theoretical modeling, Lin et al. proposed to define two factors for predicting the possibility of SSA: a thermodynamic factor ΔF and a kinetic factor κ.[6] In the proposed model, the thermodynamic factor ΔF is defined to be the Gibbs free-energy difference between the final amorphous phase and the initial multilayered films, in which the interfacial free energy is included in the calculation. Interestingly, the defined kinetic factor κ is deduced to be correlated not only with the atomic volume ratio considered in the previous models but also with the melting points of the constituent metals, indicating that both of these two parameters play a role in influencing the interdiffusion between the constituent metals.

Due to its large positive ΔH_f, being about +27 kJ/mol atom,[7] the Cu−Re system is immiscible at equilibrium and features some interesting properties. For example, some studies indicate that the Cu atoms in the Cu−Re catalysts can be significantly perturbed and such a perturbation can dramatically alter its chemical and electronic behaviors.[8] Goodman found that the carbon monoxide on Cu−monolayer/Re(0001) could be stabilized, yet it could not be stabilized in the case of bulk Cu.[9] Because of their unique chemical-absorption property, the preparation processes of the Cu−Re films have, therefore, been extensively studied. Schrebler et al. observed an amorphous phase with a cauliflower structure in the electron-deposited Cu−Re alloys.[10] In contrast, He et al. found that when the coverage thickness was less than two monolayers, Cu could form a stable and uniform layer on the Re substrate.[11] To the best of the authors' knowledge, relevant theoretical modeling at an atomic scale, concerning the SSA taking place in the Cu−Re system, has, so far, not been reported.

In the present study, we undertake molecular dynamics (MD) simulations to investigate the interfacial stability and the solid-state reaction of the Cu−Re multilayered films at an atomic scale. Since there is no equilibrium compound in the immiscible Cu−Re system, very few experimental data are available for constructing the realistic Cu−Re potential. Accordingly, before performing the MD simulations, ab intio calculations are first carried out to acquire some physical properties of a few possible Cu−Re compounds. The acquired properties are then used in fitting the Cu−Re potential, which is later applied to perform the MD simulations.

* Corresponding author. E-mail: dmslbx@tsinghua.edu.cn.

10.1021/jp052509s CCC: $30.25
Published on Web 08/10/2005

II. Methods and Procedures

A. Ab Initio Calculation. The ab initio calculations are carried out using the CASTEP of Materials Studio.[12] In the calculations, the fully nonlocal, Vanderbilt-type, ultrasoft pseudopotentials are adopted to describe the electron−ion interaction, which allows the use of a moderate cutoff for the construction of the plane-wave basis for the transition metals. The exchange and correlation items are described by the generalized-gradient approximation proposed by Perdew and Wang.[13] The precision of the calculations is set to ultrafine class. For convenience as well as feasibility, the ab initio calculations are conducted only for fcc Cu, hcp Re, $L1_2$ Cu_3Re, and $L1_2$ $CuRe_3$. The geometry optimization is first performed to determine the lattice constant and the total energy. The elastic moduli and bulk modulus of two metastable compounds (i.e., $L1_2$ Cu_3Re and $L1_2$ $CuRe_3$) are then acquired by ab initio calculations.

B. Construction of *n*-Body Cu−Re Potential. The tight-binding potential, namely the second-moment approximation of the tight-binding scheme (TB−SMA), is adopted to construct the *n*-body Cu−Re potential, as the scheme has successfully been employed in a large number of fcc and/or hcp transition metals.[14−16] In the TB−SMA scheme, the repulsive portion is a Born−Mayer pairwise interaction and the attractive portion is a second-moment approximation of the tight-binding band energy. The cohesive and repulsive items of the total energy are exponential functions of the atomic distance as written below:

$$E_{\text{total}} = \sum_i \left\{ \sum_{j \neq i} A_{\alpha\beta} \exp\left[-p_{\alpha\beta}\left(\frac{r_{ij}}{r_{\alpha\beta}} - 1\right)\right] - \sqrt{\sum_{j \neq i} \xi_{\alpha\beta}{}^2 \exp\left[-2q_{\alpha\beta}\left(\frac{r_{ij}}{r_{\alpha\beta}} - 1\right)\right]} \right\} \quad (1)$$

where α and β indicate the atomic species, r_{ij} is the distance between atoms *i* and *j*, and is calculated up to a cutoff distance r_{cutoff}, whereas $r_{\alpha\beta}$ is taken to be the nearest distance between atoms α and β in the crystal structure. $A_{\alpha\beta}$, $p_{\alpha\beta}$, $\xi_{\alpha\beta}$, and $q_{\alpha\beta}$ are adjustable potential parameters, which are generally determined by fitting them to their respective physical properties. In this study, these parameters are determined as follows. (i) For $\alpha = \beta$, the fitting procedures are performed on the cohesive energies, lattice constants, and elastic moduli at 0 K for the pure Cu and Re metals. The parameters $r_{\alpha\alpha}$ and $r_{\beta\beta}$ are taken to be the nearest-neighbor distance, i.e., r_0, of the pure Cu and Re metals, respectively. (ii) For $\alpha \neq \beta$, the corresponding parameters are fitted to the ab initio-acquired lattice constants, cohesive energies elastic, and bulk moduli of the metastable $L1_2$ Cu_3Re and $CuRe_3$ compounds.

C. Molecular Dynamics Simulation with the Cu−Re Sandwich Model. It is reported that, for an equilibrium-immiscible system characterized by a large positive ΔH_f, the interfaces consisting of the closed-packed atomic planes are frequently thermally stable, whereas those consisting of the opened atomic planes are unstable.[17] To represent the real multilayered films that may appear as solid-state amorphization in experiments, the sandwich models are constructed by stacking, along the *z*-axis, 10 fcc Cu (100) planes (No. 1−10), 12 hcp Re (01$\bar{1}$0) (No. 11−22), and 6 fcc Cu (100) planes (No. 23−32), which are arranged parallel to the *x*−*y* plane. Two interfaces thus locate at No. 10−11 and No. 22−23 atomic planes, respectively. The crystalline directions [100] of fcc Cu and [2$\bar{1}\bar{1}$0] of hcp Re with the unit distances of 3.615 and 2.760 Å, respectively, are arranged to be parallel to the *x*-axis, leading to a size difference ratio of 1.310. Meanwhile, the crystalline directions [010] of fcc Cu and [0001] of hcp Re with the unit distances of 3.615 and 4.460 Å, respectively, are arranged parallel to the *y*-axis, leading to a size difference ratio of 0.811. Considering the simulation to be under a manageable scale, the numbers of Cu and Re atoms in the *x*−*y* plane are selected to be $10 \times 10 \times 2 = 200$ atoms and $13 \times 8 \times 3 = 312$ atoms, respectively, resulting in a lattice difference ratio of 1.310 in *x*-axis and 0.81 in *y*-axis, respectively, which are reasonably close to the above-mentioned real situation. The misfits in *x*- and *y*-directions at the interface are 0.037% and 0.65%, respectively. In this regard, it has been proven that when the misfit is less than 1%, the effect of the strain on the MD simulation can be neglected.[18,19] The intervals between the Cu and Re layers in the sandwich model are set to be 1.71 Å so that the sandwich model energy curve has a minimum interval at the optimized distance. In the three directions, periodic conditions are employed and the two Cu lattices in the model are, therefore, adhered together to form a united lattice. There are a total of 4000 Cu atoms and 1248 Re atoms in the sandwich model. It has been shown, in experiments, that the interface between two metal−metal layers is frequently a transient layer, in which the atoms possess higher energy than that of the atoms in the bulk form and that the thickness of the transient layer is about 2−8 Å.[20,21] Accordingly, in setting up the sandwich models, chemical disordered interlayers are artificially introduced by randomly exchanging an equal number of Cu and Re atoms at the layers close to the interfaces, resulting in a long-range order (LRO) $\eta = 0.5$. The LRO is defined as $\eta = (p - \gamma)/(1 - \gamma)$, where *p* and γ are the probability of the presence of an *A*-type atom on its own lattice site and the molar ratio of *A* atoms, respectively. Accordingly, values $\eta = 0$ and 1 correspond, respectively, to a complete chemical disorder and entirely ordered states.[18]

After exchanging the Cu and Re atoms, MD simulation is carried out for the sandwich model using the Parrinello−Rahman constant pressure scheme and the equations of motion are solved through a fourth-order predictor−corrector algorithm of Gear with a time step of $t = 5 \times 10^{-15}$ s.[22,23] The sandwich model is running at 300 K for 8×10^6 MD steps (40 ns) to reach a relatively stable state, at which all the related dynamic variables show no secular variation. The process of structural change in the sandwich models is monitored by the pair-correlation functions $g(r)$. To calculate the $g(r)$, each atom was imagined to be at the center of a series of concentric spheres. The atomic density $\rho(r)$ was defined to be the number of atoms in each spherical shell divided by the volume of that shell, with the consideration of those periodic images located outside the block. By averaging all the atoms within 200 time steps, the $g(r)$ can then be obtained by the following formula:

$$g(r) = \frac{\rho(r)}{\rho_0} \quad (2)$$

where $\rho(r)$ denotes the atomic density at $r = |r|$, $r = 0$ defines the position of a reference atom, and ρ_0 is an average atomic density for the entire model. The density profiles $\rho_\alpha(z)$ of each species along the *z*-direction are also inspected to provide evidence of the structural changes of interest.[24]

III. Results and Discussion

A. Ab Initio Calculations and Construction of *n*-Body Cu−Re Potential. We first present the results of ab initio

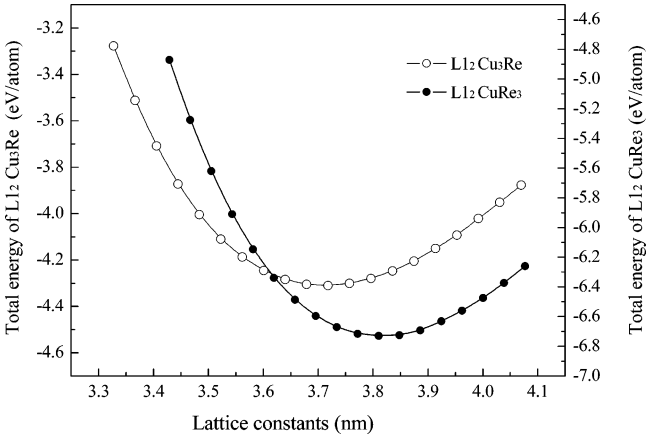

Figure 1. Correlations between the lattice constants and the total energy of $L1_2$, Cu_3Re, and $CuRe_3$ determined by ab initio calculations.

calculations for the $L1_2$ Cu_{3Re} and $CuRe_3$ metastable compounds. Figure 1 shows the correlations between the lattice constants of the two metastable compounds and their total energies obtained from ab initio calculations. From Figure 1, it can be determined that the lattice constants of the two compounds are 0.369 and 0.381 nm, respectively. Using the total energies of Cu and Re, the formation energies of the two compounds are calculated to be 0.315 and 0.165 eV, respectively.

To investigate the stability of the two Cu−Re metastable compounds at low temperature, MD simulations were performed, based on the constructed *n*-body Cu−Re potential, at 50 K and zero pressure. It turned out that the two Cu−Re compounds could be sustained in a metastable state at low temperature. Consequently, the physical properties of the two metastable Cu−Re compounds can be used to fit the *n*-body potential. Table 1 lists the physical properties, such as the lattice constants and the formation energies, of the $L1_2$ Cu_3Re and $L1_2$ $CuRe_3$ compounds determined by ab initio calculations and/or by experimental measurements. One can see that the formation energies of the Cu_3Re and $CuRe_3$ compounds predicted by the Miedema theory[27] are 0.28 and 0.17 eV/atom, respectively. Since the formation energies of the Cu_3Re and $CuRe_3$ compounds are both positive, they are both unstable in an equilibrium state, which is in good agreement with the fact that the Cu−Re system is immiscible at equilibrium. Generally speaking, the values obtained from thermodynamic and ab initio calculations are consistent with each other. For convenience of comparison later, the elastic moduli of the Cu−Re alloys were also determined by ab initio calculations.

Using the data in the Table 1 and the procedure described above, the TB−SMA potential can be derived for the Cu−Re system. The TB−SMA potential parameters for the Cu−Re system are listed in Table 2. To test the relevance of the potential, the elastic moduli of the Cu−Re system are reproduced from the constructed potential and compared with those obtained from ab initio calculations or from experiments. From Table 1, it is obvious that the physical properties fitted to or reproduced from the derived *n*-body potential agree well with those obtained from ab initio calculations and/or the experimental results.

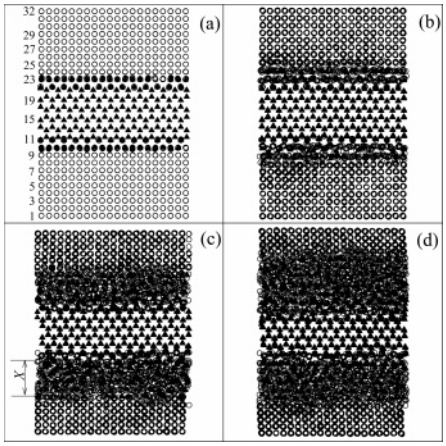

Figure 2. Projection of the atomic position on the $x-z$ plane of the sandwich model at the initial state (a) and the annealing states at 300 K for (b) 0.05, (c) 10, and (d) 30 ns, respectively.

TABLE 2: Tight-Binding Potential Parameters of the Cu−Re System Constructed in the Present Study[a]

	p	*q*	*A*	*ξ*
Cu−Cu	10.5654	2.4251	0.0881	1.3284
Re−Re	16.7080	2.2823	0.1069	2.6918
Cu−Re	11.3178	2.5865	0.1729	2.3297

[a] A and ξ are expressed in eV.

B. Solid-State Amorphization in the Cu−Re System. We now present the detailed simulation results observed in the Cu−Re sandwich model. Figure 2 displays four projections of the atomic positions on the $x-z$ plane of the initial state and after isothermally annealing for 0.05, 10, and 30 ns. The projections exhibit vividly the process of solid-state amorphization taking place in the Cu−Re sandwich model. Figure 2a shows the initial state of the sandwich model, in which some chemical disordering is present at the interface in order to simulate the real situation that, in practice, a disordered interlayer could be formed at the Cu/Re interface. After simulation for 0.05 ns, Figure 2b shows that the majority of the atoms far from the interface in the sandwich model still retain their crystalline structure as in the initial state, whereas those atoms near the interface change into a disordered state, indicating that solid-state amorphization is taking place at the interface. Further increasing the simulation time to 10 and 30 ns, the amorphous interlayer gradually grows as seen in Figure 2c,d.

TABLE 1: Comparison of the Physical Properties of fcc Cu, hcp Re, $L1_2$ Cu_3Re, and $L1_2$ $CuRe_3$ Obtained from Ab Initio Calculations, Fitted, or Reproduced from *n*-Body Potentials and the Experimental Observation[25−27,a]

		a	c	E_f	E_c	C_{11}	C_{12}	C_{13}	C_{33}	C_{44}
fcc Cu	experimental	0.361			3.49	1.683	1.221			.757
	reproduced	0.361			3.60	1.853	1.131			0.723
hcp Re	experimental	0.276	0.446		8.03	6.182	2.753	2.078	6.835	1.606
	reproduced	0.274	0.448		8.04	6.525	2.571	2.143	6.831	1.558
$L1_2$ Cu_3Re	CASTEP	0.369		0.315		2.502	1.774			0.931
	reproduced	0.374		0.315		2.337	1.542			1.004
$L1_2$ $CuRe_3$	CASTEP	0.381		0.165		4.127	2.716			1.573
	reproduced	0.376		0.165		4.701	3.133			1.733

[a] Lattice constants a and c are expressed in nm. Elastic moduli C_{ij} are expressed in MBar. Cohesive energies E_c and formation energies E_f are expressed in eV.

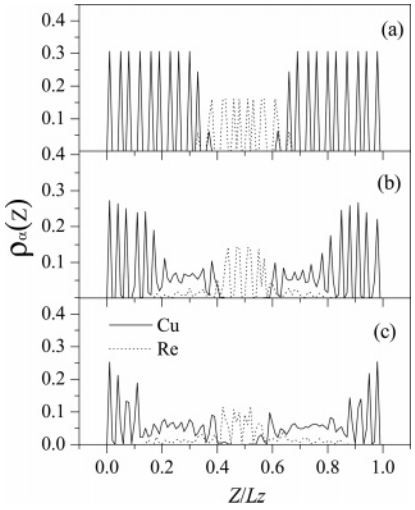

Figure 3. Density profiles $\rho_\alpha(Z)$ of Cu (solid line) and Re (dashed line) along the *z*-direction at the initial state (a) and the annealing states at 300 K for (b) 10 and (c) 30 ns, respectively.

By carefully inspecting Figure 2, one can see that the amorphous interlayer grows in a layer-by-layer mode, which is evidenced by the following calculated density profiles as a function of simulation time. Figure 3 shows the change of the Cu and Re atomic density profiles $\rho_\alpha(z)$ along the *z* direction, perpendicular to the interface, with increasing MD simulation time steps. Figure 3a is the initial state of the sandwich model from which a perfect layered structure can be seen. Figure 3b shows that after MD simulations up to about 10 ns, some Re (Cu) atoms near the interface diffuse into the partner Cu (Re) lattice and thus result in interfacial amorphization. However, one can note that, in the areas far away from the interface, the Cu and Re lattices still retain their respective crystalline structures. It can be seen in Figure 3c,d that after running up to 10 and 30 ns, more and more atoms diffuse into their partner lattices and that more crystalline planes, especially fcc Cu crystalline planes, turn into the disordered state. To give a decisive confirmation of the layer-by-layer growing mode, the total pair correlation $g(r)$ of each atomic plane was calculated after running 0, 0.05, and 30 ns. Figure 4 displays three sets of calculated $g(r)$ for the atomic planes 1, 7, and 16, respectively, at three times. Figure 4a shows that at the initial state, the three atomic planes are all of crystalline structure, corresponding to fcc Cu and hcp Re, respectively. At 0.05 ns, one can see, from Figure 4b, that atomic plane 7 has turned into an amorphous state; however, the atomic planes far away from the interface (e.g. planes 1 and 16) keep the same features as their original crystalline structures. After running for 30 ns, Figure 3c shows that the fcc Cu crystalline plane 3 also becomes disordered, whereas the atomic plane 16 still keeps its crystalline structure. On the basis of the above description, it can be concluded that the solid-state amorphization grows in a layer-by-layer mode.

From Figures 2−4, one can also observe that the solid-state amorphization in the Cu−Re system features a so-called asymmetric-growth behavior, that is, the disordered interlayer extends faster toward the Cu lattice than toward the Re direction. For example, Figure 2c shows that after running 10 ns, more than three atomic planes of Cu lattice have become disordered, whereas only two atomic planes of Re have become amorphous. Since the cohesive energy of Re is larger than that of Cu, the Re lattice is thought to be more stable than the Cu lattice. One can, therefore, consider that the Re lattice is more difficult to turn into a disordered state. In fact, the asymmetric-growth has frequently been observed in solid-state amorphization of transition metal−metal systems, such as in the Ni−Mo, Ni−Nb, and Ni−Zr systems.[28−30]

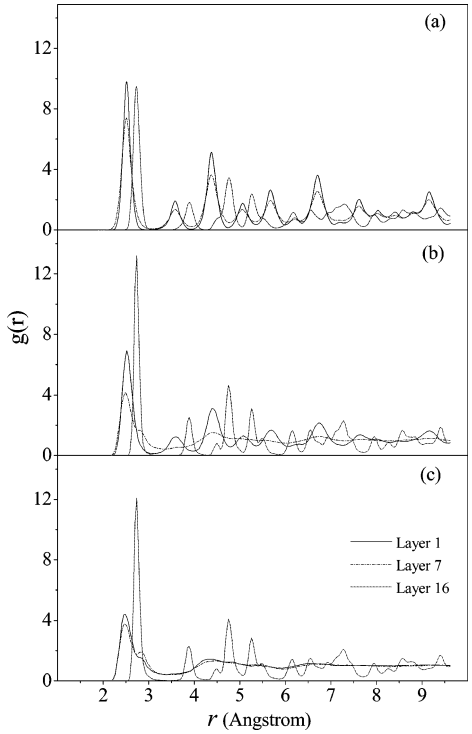

Figure 4. Total pair-correlation functions $g(r)$ of layers 1, 3, and 9 at the initial state (a) and the annealing states at 300 K for (b) 0.05 and (c) 30 ns, respectively.

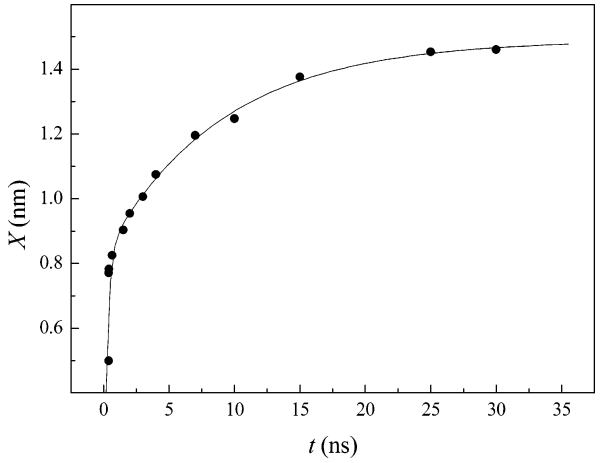

Figure 5. Thickness *X* of amorphous interlayer as a function of the isothermal annealing time *t*.

We now turn to discuss the detailed growth kinetics of the solid-state amorphization in the Cu−Re sandwich model. MD simulation shows that, with increasing the simulation time, the growing speed of the amorphous interlayer gradually slows down and eventually approaches zero. Figure 5 shows the correlation of the thickness of the amorphous interlayer to the simulation time. From Figure 5, one can see that the growth of the amorphous interlayer can be divided into three stages: (i) the fast nucleating stage, (ii) the diffusion-growing stage, and (iii) the steady finishing stage. In the first stage, due to the very high interfacial energy as well as the very short distance covered by the diffusing of Cu and Re atoms, many nuclei of the amorphous phase form and quickly grow in the interface, resulting in a fast growth of the amorphous interlayer. In the fast nucleating stage, which lasts about 0.01−0.05 ns, the

TABLE 3: Thermodynamics Parameters of Miedema's Model and Alonso's Method[7] Used in Calculation for the Thermodynamic Factor ΔF and the Kinetic Factor κ of the Cu−Re System

	V (cm^3)	ϕ^* (V)	n_{ws} (density unit)	ΔH^{fuse} (kJ/mol)	T (K)	γ^0 (mJ/m^2)	κ	ΔF (kJ/mol)	Λ_{max} (nm)
Cu	7.11	4.45	3.18	13.00	1358	1825	6.6	−8.23	1.35
Re	8.85	5.20	6.33	33.25	3453	3453			

amorphous interlayer grows up to about 3−7 Å. At this stage, the governing factor is the nucleation of the amorphous phase. Subsequently, the amorphous interlayer comes into the diffusion-growing stage, lasting about 20 ns, in which the amorphous interlayer grows to about 13−14 Å. In this stage, the atomic diffusion plays a governing role. With the atoms diffusing as well as the interlayer growing, the interfacial energy is reduced to a lower and lower level. Accordingly, the driving force of the solid-state amorphization becomes weaker and weaker and, therefore, the growing speed of the amorphous interlayer gradually slows down to zero. At this moment, the growth of the amorphous interlayer almost terminates and, therefore, comes into a steady finishing stage. In this stage, the thickness of the amorphous interlayer remains almost unchanged. For example, after further running from 30 to 80 ns (i.e., to 8×10^6 MD time steps), no observable change can be detected. Note that after the termination of the solid-state amorphization, there are still crystalline Cu and Re lattices remaining outside the newly formed amorphous layer, suggesting that there is no adequate driving force for further growth of the amorphous interlayer. From Figure 5, one can estimate the maximum thickness of the amorphous interlayer (about 1.47 nm), at which the growing speed is about zero, i.e., SSA is terminated.

C. Thermodynamic Calculation on SSA in the Cu−Re System. In this section, we further discuss the solid-state amorphization in the immiscible Cu−Re multilayers from the thermodynamic as well as the kinetic points of view. According to the model proposed by Lin et al., two necessary conditions have to be satisfied for the solid-state amorphization to take place in a binary-metal system.[6] First, the formed amorphous phase should have a lower Gibbs free energy than the initial energetic state of the multilayers, i.e., the thermodynamic factor ΔF, defined as the energy difference between the amorphous phase and the multilayers, should be negative. Second, the kinetic factor κ should be greater than 0.6 for a transition metal−metal system. According to the definitions, the thermodynamic factor ΔF and the kinetic factor κ can be respectively expressed by

$$\Delta F = \Delta G_{\{AB\}} - 2\left(\gamma_{[A]-\{AB\}} + \gamma_{[B]-\{AB\}} + d_{AB}\frac{\Delta G_{\{AB\}}}{V_{\{AB\}}}\right)\frac{V_{\{AB\}}}{(D_A + D_B)} \quad (3)$$

$$\kappa = 1 - \frac{V_A^{eff}}{V_B} + (T_B - T_A)\left(\frac{1}{T} - \frac{1}{T_B}\right) \quad (4)$$

where $\Delta G_{\{AB\}}$ is the difference of Gibbs free energies between the amorphous state and the crystalline state of the $A-B$ alloy (A and B stand for the constituent metals). $\gamma_{A-\{AB\}}$ and $\gamma_{B-\{AB\}}$ are the interfacial free energies of the $A-\{AB\}$ and $B-\{AB\}$ interface, respectively. D_A and D_B are the thicknesses of the A and B layers, respectively. d_{AB} is the growing thickness of the amorphous interlayer. $V_{\{AB\}}$ is the mean value of the atom volumes of A and B, and V_A^{eff} is the effective volume of A in the matrix of the metal B. T, T_A, and T_B are the annealing temperature and the melting points of metals A and B, respectively. Concerning the definitions and calculation of those variables, the readers are referred to the published literature.[6,31] From eq 3, by setting $F = 0$, one can obtain the following equation to estimate the maximum thickness of the growing amorphous interlayer:

$$\Lambda_{max} = \frac{(\gamma_{[A]-[AB]} + \gamma_{[B]-[AB]})V_{\{AB\}}}{\Delta G_{\{AB\}}} \quad (5)$$

Substituting the relevant quantities of the Cu−Re system into the above equation, one can obtain that the thermodynamic factor ΔF, the kinetic factor κ, and the maximum thickness of amorphous interlayers of the Cu−Re system are −8.23 kJ/mol, 6.6, and 1.35 nm, respectively. Table 3 lists the calculated results and the parameters used in the calculation. From Table 3, one can clearly see that the thermodynamic factor ΔF is truly negative and the kinetic factor κ is greater than 0.6, suggesting that the solid-state amorphization is able to take place in the Cu−Re system. Interestingly, the maximum thickness of the amorphous interlayers is calculated to be 1.35 nm.

It should be noted that in the thermodynamic calculation, those variables are adopted from averaged values obtained from experiments, while in MD simulations, the interface consists of the open atomic planes, of which the interfacial energy is higher than the averaged values used in thermodynamic calculation. It can be deduced that the maximum thickness of the amorphous interlayer should be greater than the above estimated 1.35 nm. In other words, the result from thermodynamic calculation is fairly compatible with the prediction from the above MD simulations based on the newly derived n-body Cu−Re potential.

IV. Summary and Remarks

An n-body Cu−Re potential is constructed under the second-moment approximation of a tight-binding scheme and is of proven relevance in reflecting the interatomic interaction of the Cu−Re system. Based on the constructed Cu−Re potential, molecular dynamics simulations using the Cu−Re sandwich model reveal that the solid-state amorphization can take place in the interface of the Cu−Re multilayers and that the amorphous interlayer grows in a layer-by-layer mode, featuring an asymmetric behavior. It is also found that, with increasing the simulation time, the growth speed of the amorphous interlayer slows down gradually and eventually becomes zero and that the maximum thickness of the interlayer is about 1.47 nm, which is compatible with the estimated value from the thermodynamic calculation.

Acknowledgment. The authors are grateful for the financial support from the National Nature Science Foundation of China, the Ministry of Science and Technology of China (G20000672), and the Administration of Tsinghua University.

References and Notes

(1) Schwarz, R. B.; Johnson, W. L. *Phys. Rev. Lett.* **1983**, *51*, 415.
(2) Clemens, B. M. *Phys. Rev. B* **1986**, *33*, 7615.
(3) Zhang, Z. J.; Liu, B. X. *Appl. Phys.* **1994**, *76*, 3351.
(4) Pan, F.; Chen, Y. G.; Liu, B. X. *Appl. Phys. Lett.* **1995**, *67*, 780.
(5) Chen, Y. G.; Liu, B. X. *J. Phys. D* **1997**, *30*, 1729.
(6) Lin, C.; Yang, G. W.; Liu, B. X. *Phys. Rev. B* **2000**, *61*, 15649.
(7) Miedema, A. R.; Niessen, A. K.; et al. *Cohesion in Metals: Transition Metal Alloys*; North-Holland: Amsterdam, 1989.
(8) Rodriguez, J. A.; Campbell, R. A.; Goodman, D. W. *Surf. Sci*. **1991**, *244*, 211.
(9) Rodriguez, J. A.; Campbell, R. A.; Goodman, D. W. *J. Vac. Sci. Technol. A* **1991**, *10*, 2540.

(10) Schrebler, R.; Merino, M.; Cury, P.; Romo, M.; Cordova, R.; Gomez, H.; Dalchile, E. A. *Thin Solid Films* **2001**, *388*, 201.
(11) He, J. W.; Goodman, D. W. *J. Phys. Chem*. **1990**, *94*, 1502.
(12) Vanderbilt, D. *Phys. Rev. B* **1990**, *41*, R7892.
(13) Perdew, P.; Wang, Y. *Phys. Rev. B* **1992**, *45*, 13244.
(14) Ducastelle, F. In *Computer Simulation in Materials Science;* Meyer, M., Pontikis, V., Eds.; NATO Advanced Study Institute, Series E, Applied Physics, Vol. 205; Kluwer: Dordrecht, 1991.
(15) Cleri, F.; Rosato, V. *Phys. Rev. B* **1993**, *48*, 22.
(16) Rosato, V.; Guillope, M.; Legrand, B. *Philos. Mag. A* **1989**, *59*, 321.
(17) Gong, H. R.; Liu, B. X. *Appl. Phys. Lett*. **2003**, *83*, 4515.
(18) Massobrio, C.; Pontikis, V.; Matin, G. *Phys. Rev. B* **1990**, *41*, 10486.
(19) Mura, P.; Demontis, P.; Suffritti, G.; Rosato, V.; Antissari, M. *Phys. Rev. B* **1994**, *50*, 2850.
(20) Bai, J. M.; Fullerton, E. E.; Amontano, P. A. *Phys. B* **1996**, *221*, 411.
(21) Chushkin, Y.; Jergel, M.; Luby, Š.; Majková, E.; Ožvold, M.; Kuwasawa, Y.; Okayasu, S.; D'Anna, E.; Luches, A.; Martino, M. *Appl. Surf. Sci*. **2005**, *243*, 62.
(22) Parrinello, M.; Rahman, A. *J. Appl. Phys*. **1981**, *52*, 7182.
(23) Allen, M. P.; Tildesley, D. J. *Computer Simulation of Liquids*; Oxford University Press: Oxford, 1987.
(24) Rosato, V.; Ciccotti, G.; Pontikis, V. *Phys. Rev. B* **1986**, *33*, 1860.
(25) Pearson, W. B. *A Handbook of Lattice Spaces and Structures of Metals and Alloys*; Pergamon: London, 1958.
(26) Brandes, E. A.; Brook, G. B. *Smithells Metals Reference Book*, 7th ed.; Butterworth−Heinemann: Oxford, 1992.
(27) Lide, D. R. *Handbook of Lattice Spaces and Structures of Metals and Alloys*; CRC: New York, 2002.
(28) Zhang, Z. J.; Liu. B. X. *J. Appl. Phys*. **1994**, *76*, 3351.
(29) Zhang, Q.; Lai, W. S.; Liu, B. X. *Phys. Rev. B* **1998**, *58* 14020.
(30) Dai, X. D.; Li, J. H.; Liu, B. X. *J. Phys. Chem. B* **2005**, *109*, 4717.
(31) Liu, B. X.; Lai, W. S.; Zhang, Z. J. *Adv. Phys*. **2001**, *50*, 367.